the IBV (Panel a) into a weak but wide filament (Panel c), while the present analysis has corrected its position (Panel d) and its temperature to ~23.5–24°C, as given by the satellite image. An issue here is that the OI imposes uniform scaling parameters, independently of the local dynamics. One may argue that the dynamical evolution subsequent to the OI assimilation could ''repair'' the OI fields. However, this adjustment is carried out at dynamical time-scales, which may be too slow. The main methodological result of the above intercomparisons is that the present analysis improves the OI one and compares well with SST nowcast.

3.2.1.2. Nonlinear forecast of the dominant error covariances. Fig. 13 deals with the convergence of the forecast of the dominant error covariance matrix for Sept. 18. Panel (a) shows the history of the similarity coefficient ρ (Section A.4, Eq. (A28)) which

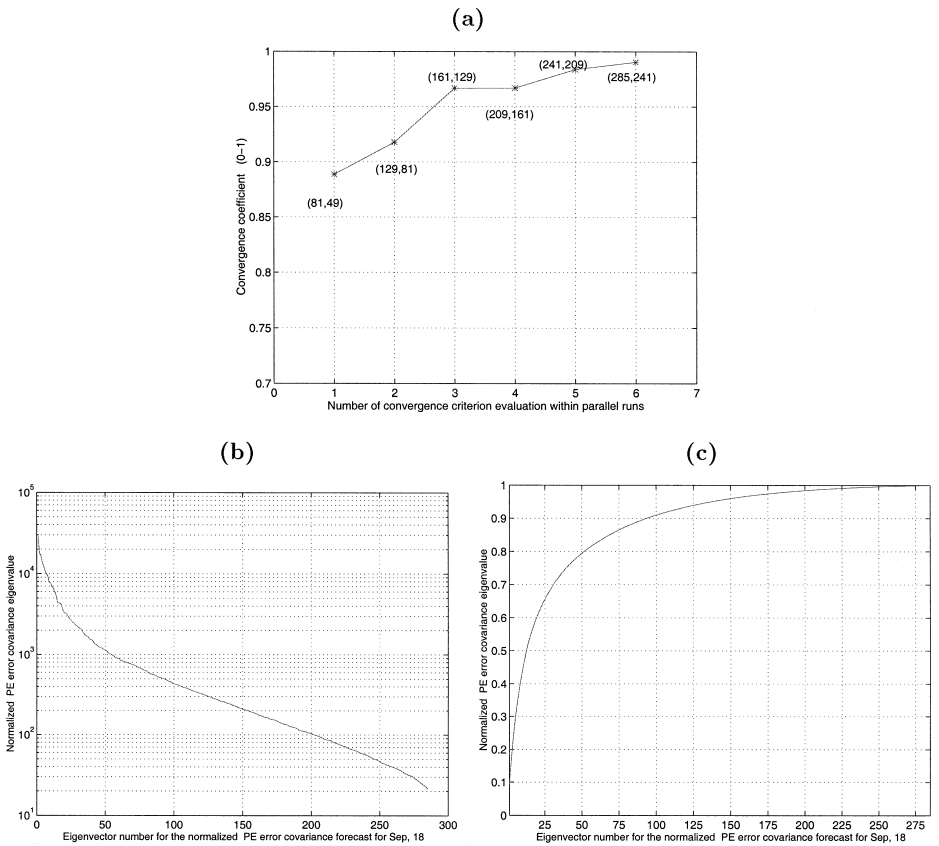

Fig. 13. Panel (a) shows the values of the similarity coefficient ρ of the ES forecast for Sept. 18. With the ensemble sizes 285 (current) and 241 (previous), ρ was 99.05%, higher than the 99% limit chosen. Parallel iterations were thus stopped. Panel (b) is the eigenvalue spectrum of the normalized ES covariance forecast for Sept. 18. Panel (c) is the cumulative (0–1) spectrum associated with (b). Utilizing 50 error eigenvectors already accounts for 80% of the variance explained by the 285 vectors; using 100 vectors accounts for 90% of that variance.